Differences and Similarities of High-resolution Computed Tomography Features Between Pneumocystis Pneumonia and Cytomegalovirus Pneumonia in Aids Patients

Chunjing Du
Capital Medical University Affiliated Beijing Ditan Hospital
Jingyuan Liu
Capital Medical University Affiliated Beijing Ditan Hospital
Hui Chen
Capital Medical University Affiliated Beijing Ditan Hospital
Shuo Yan
Capital Medical University Affiliated Beijing Ditan Hospital
Lin Pu
Capital Medical University Affiliated Beijing Ditan Hospital
Haofeng Xiong
Capital Medical University Affiliated Beijing Ditan Hospital
Pan Xiang
Capital Medical University Affiliated Beijing Ditan Hospital
Chuansheng Li
Capital Medical University Affiliated Beijing Ditan Hospital
Ming Zhang
Capital Medical University Affiliated Beijing Ditan Hospital
Budong Chen
Capital Medical University Affiliated Beijing Ditan Hospital
Ang Li (liang@ccmu.edu.cn)
Capital Medical University Affiliated Beijing Ditan Hospital

Research Article

Keywords: Diagnostic imaging, Pneumonia, HIV/AIDS

Posted Date: June 16th, 2020

DOI: https://doi.org/10.21203/rs.3.rs-34736/v1

Version of Record: A version of this preprint was published on October 26th, 2020. See the published version at https://doi.org/10.1186/s40249-020-00768-2.

Abstract

Background: Accurate differentiating diagnosis of pneumocystis pneumonia and cytomegalovirus pneumonia is crucial for choosing therapies in AIDS patients. Hence, the purposes of this study was to compare the CT features of pneumocystis pneumonia and cytomegalovirus pneumonia in AIDS patients and to spot the valuable findings which might contribute to an accurate diagnosis between two cohorts.

MethodsA total of 112 AIDS patients, 78 withpneumocystis pneumoniaand 34 werecytomegalovirus pneumonia,were included in this study.Two experienced chest radiologists retrospectively reviewed CT images for 17 features including ground-glass opacity, consolidation, nodules, and halo sign. Significance was calculated by the chi-square($\chi 2$)test.

ResultsThe presence of consolidation (61.77% in cytomegalovirus pneumonia,35.9% in pneumocystis pneumonia, p=0.011), halo signs (32.35% in cytomegalovirus pneumonia, 11.54% in pneumocystis pneumonia, p□0.001), and nodules (47.06% in cytomegalovirus pneumonia,8.97% in pneumocystis pneumonia, p□0.001), especially small nodules (32.5% in cytomegalovirus pneumonia, 6.41% in pneumocystis pneumonia, p□0.001) without perilymphatic distribution,was significantly more frequent in patients with cytomegalovirus pneumonia than in those with pneumocystis pneumonia. Large nodules were not found in any of patients with cytomegalovirus pneumonia. The presence of ground-glass opacity (100% in pneumocystis pneumonia and cytomegalovirus pneumonia), reticulation(57.69% in pneumocystis pneumonia, 52.94% in cytomegalovirus pneumonia, p=0.782) andbronchial wall thickening (34.62% in pneumocystis pneumonia, 47.06% in cytomegalovirus pneumonia, p=0.213) were common in both groups.

ConclusionsAnalysis of consolidation, nodules, and halo signs may contribute to prioritize differential diagnosis of pneumocystis pneumonia or cytomegalovirus pneumonia. However, some CT features considered typicalin oneor other diseases appear with similar frequency in both cohorts of AIDS patients.

Background

The infectious diseases remain a major burden of global health concern in resource-poor settings, especially the emerged novel coronavirus disease 2019 and the widespread HIV/AIDS[1, 2]. Pneumocystis pneumonia (PCP) and cytomegalovirus pneumonia (CMV-P) are the most common infectious complications in patients with AIDS and other immunodeficiencies[3, 4]. Untreated, the mortality of PCP up to 100%. Even with therapy, the mortality approaches 10–20% [5]. The incidence of CMV-P is 20%-35% and the mortality of exposed patients is high, up to 70%, especially when diagnosis is delayed [6, 7]. Both types of pneumonia have similar clinical symptoms and signs, including fever, unproductive coughing, hypoxemia, and dyspnea. Therapeutic strategies are different due to characteristics of infected pathogens. Thus, identifying the pathogenic agent is crucial for diagnosing and initiating appropriate therapies regarding causative pathogens.

The diagnosis of PCP and CMV-P is usually established with identification of P. jiroveci and cytomegalovirus inclusion bodies in lung biopsy or sensitive immunocytochemical methods in bronchoalveolar lavage (BAL) fluid[8–11] .

Despite current advances in diagnostic methods, the diagnosis of both types of pneumonia is challenging. Microbiological confirmation is frequently invasive or difficult to obtain, which may have delayed the diagnosis and initiation of therapies[12]. In addition, the absence of microbiological evidence and negative results of serum antibodies are not reliable evidence to rule out pulmonary infection [13]. Imaging, especially high-resolution computed tomography (HRCT), which is fast, non-invasive, and more specific and sensitive than X-rays in detecting early or tiny lesions, represents a vital tool for guiding the diagnosis in patients with pneumonia and plays a pivotal role in monitoring the therapeutic effect [14]. To our knowledge, no study has specifically compared HRCT features between PCP and CMV-P in AIDS patients. Thus, it is essential to incorporate the radiographic features into clinical information so as to narrow the differential diagnosis appropriately.

The purpose of this study was to compare pulmonary HRCT features of PCP and CMV-P in AIDS patients and to spot the valuable findings which might contribute to an accurate diagnosis for patients' further management.

Methods

Patients

Our institutional ethics committee approved this study and informed consent was waived because of its retrospective nature. HRCT scans were reviewed in 112 AIDS patients with confirmed PJP and CMV-P treated at Beijing Ditan Hospital from January 2017 to May 2019. All patients received bronchoscopy and performed serological and bacteriological examinations, and cases with existing co-infections were excluded from this study. The study comprised 78 patients with PJP and 34 patients with CMV pneumonia. A diagnosis of PJP was confirmed when symptoms of infection (fever, cough with or without sputum, leukocytosis or leukopenia) coinciding with identification of P. jiroveci by silver stain or PAS in a bronchoscopy specimen. CMV-P cases were established when detailed clinical evidence for infection (fever, cough with or without sputum, leukocytosis or leukopenia) coinciding with definitive BAL results of fluorescence quantitative PCR. The evaluated HRCT images were selected from the closest to the date of diagnostic BAL.

Ct Examinations

The thorax HRCT examinations were performed on a 256-detector row spiral CT scanner (Philips, iCT, Holland), or a 64-detector row spiral CT scanner (GE, Lightspeed VCT, USA). The HRCT scans were performed at end-inspiration with the patient in a supine position and images were reconstructed by a

high spatial resolution algorithm. Scanning parameters for spiral CT were set to 220 automatic currents and 120 kV of energy on the basis of body weight. Images were obtained at 5 mm intervals and 5-mm thickness, with pitch of 1.0 (it) and 0.8 (VCT) throughout the chest using 0.625 mm or 1.0 mm collimation. Images were inspected at window settings that suitable for assessing lung parenchyma (level: 600–700 HU; width: 1000–1500 HU) and mediastinum (level: 30–40 HU; width: 400–500 HU).

Interpretation Of Images

The CT images were reviewed independently in a random order by two experienced chest radiologists blinded to any knowledge of the patients' clinical information. Final conclusions on the features were reached by unanimous consensus.

CT features were categorized as (a) consolidation; (b) ground-glass opacity (GGO); (c) mosaic perfusion; (d) crazy-paving pattern; (e) nodule; (f) tree-in-bud sign (TIB); (g) halo sign; (h) bronchial wall thickening; (i) reticulation; (j) mediastinal /hilar lymph node (LN) enlargement; (k) pleural effusion; (l) cavity; and (m) cyst.

GGO appeared as an area of hazy increased opacity without obscuration of bronchial and vascular margins. Consolidation appeared as an area of increased attenuation that obscured the margins of underlying vascular. When a consolidation or a GGO was both presented in an image, the predominance of the consolidation or GGO (Cons/GGO predominance) was recorded as consolidation predominance, GGO predominance, or equal predominance and their distribution was classified as segmental, non-segmental, or lobular. The crazy-paving pattern appeared as any superimposition of the intralobular interstitial or interlobular thickening within the GGO. The mosaic pattern was defined as patchwork of regions of inhomogeneous attenuation. Nodules were defined as a rounded or irregular opacity with well or poorly defined. The size of nodules was classified as micro (< 3 mm), small (3–10 mm), or large (> 10 mm) and their distribution were recorded as perilymphatic, centrilobular, or random. The tree-in-bud sign (TIB) represented centrilobular branching structures that similar to a budding tree. The halo sign was a GGO surrounding a nodule or mass.

Statistical analysis

The data were analyzed using SPSS 19.0 software package (SPSS Institute, Chicago IL, USA). Normally distributed variables were conducted using the Student's t-test. Non-normally distributed variables were compared by the Kruskal-Wallis test. Categorical variables were conducted by the Fisher's exact test and the chi-square ($\chi 2$) test. Binary logistic regression analyses were conducted to identify the significant parameters that distinguished PCP from CMV-P. Correlations were analyzed by means of Pearson or Spearman correlation analyses. The result was considered as significant in the case of a p-value < 0.05.

Results

Patients

The characteristics of patients were shown in Table 1. No differences in age, gender, weight, and transmission route ($p > 0.05$) were found in PCP and CMV-P cohort. In terms of inflammation, there was no significant difference in leukocyte counts ($p = 0.22$) and C-reactive protein ($p = 0.75$) between both groups, however, the neutrophil percentage in PCP was higher than in CMV-P group ($p = 0.01$), and the lymphocyte percentage in CMV-P was higher than in PCP group ($p = 0.02$). In addition, the HIV viral loads in PCP were significantly higher in PCP than in CMV-P ($p = 0.02$) while no differences were found in $CD4^+$T cell counts ($p = 0.28$), $CD8^+$T cell counts ($p = 0.54$), and CD4/CD8 ratio ($p = 0.48$) between two cohorts.

Table 1
Characteristics of AIDS patients with PCP and CMV-P.

	PCP (n = 78)	CMV-P (n = 34)	P-value
Age (years), median (IQR)	33 (29, 45.25)	38 (29, 48.25)	0.12
Male, n (%)	75 (96.15)	33 (97.06)	0.81
Weight (kg), mean(SD)	64.05 (11.20)	62.82 (9.99)	0.58
Transmission route, n (%)			0.41
Homosexual	25 (32.05)	12 (35.29)	
Heterosexual	9 (11.54)	1 (2.94)	
Intravenous drug	1 (1.28)	0	
Blood transfusion	3 (3.85)	1 (2.94)	
Unknown	40 (51.28)	20 (58.82)	
Leukocyte count ($\times 10^9$/L), median (IQR)	5.50 (3.64, 8.57)	4.52 (3.20, 6.85)	0.22
Neutrophil percentage(%), median (IQR)	79.39 (61.08, 86.42)	68.15 (56.18, 79.50)	0.01
Lymphocyte percentage (%),median (IQR)	11.91 (8.48, 19.54)	18.20 (12.10, 27.24)	0.02
CRP (mg/L), median (IQR)	12.65 (3.40, 36.23)	13.30 (2.70, 35.23)	0.75
HIV viral load $\log_{10}$ (copy/ml), median (IQR)	5.50 (5.17, 5.93)	5.19 (4.51, 5.67)	0.02
CD4 T cell count (cells/ul), median (IQR)	22 (9, 47.75)	22.50 (13, 77)	0.28
CD8 T cell count (cells/ul), median (IQR)	458 (329.75, 679)	485.50 (323.75, 779.50)	0.54
CD4/ CD8 ratio (%), median (IQR)	0.05 (0.02, 0.10)	0.06 (0.02, 0.16)	0.48

PCP = pneumocystis pneumonia, CMV-P = pneumocystis pneumonia, CRP = C-reactive protein, IQR = median (interquartile range), SD = standard deviation.

Ct Features Between Pcp And Cmv-p

Thoracic CT features of the 112 patients were shown in Table 2 and Table 3. We observed that GGO was common in AIDS patients with PCP and CMV-P(Figs. 1 and 3), the frequency of GGO was 100% in both cohorts. Relatively, the frequency of cavity was rare in PCP (2.56%) and CMV-P (0%). No significant differences were found in mosaic perfusion (p = 0.78), crazy-paving pattern (p = 0.98), TIB (p = 0.98), bronchial wall thickening (p = 0.48), reticulation (p = 0.48), LN enlargement (p = 0.48), cavity (p = 0.48),

and cyst (p = 0.48) between two cohorts. As shown in Table 3, the frequency of consolidation and nodules were significantly higher in patients with CMV-P than in those with PCP (p = 0.01and p□0.001, respectively) (Figs. 1, 2, 4 and 5). Compared to patients with PCP, large nodules plus perilymphatic distribution were not found in any of patients with CMV-P. In addition, halo sign was seen more often in CMV-P (32.35%) than in PCP (11.54%). To identify the significant parameters that distinguished PCP from CMV-P, binary logistic regression analyses were conducted and identified 2 meaningful parameters, including consolidation (p = 0.020; OR, 3.015; 95% CI, 1.190–7.637) and nodules (p < 0.001; OR, 9.298; 95% CI, 3.191–27.095) (Table 4). Combining consolidation and nodules, the AUC for differentiating PCP from CMV-P was 0.769.

Table 2
Thoracic CT features without significant differently frequency.

	PCP (n = 78)	CMV-P (n = 34)	P-value
GGO, n (%)	100	100	NS
Mosaic perfusion, n (%)	25 (32.05)	10 (29.41)	0.78
Crazy-paving pattern, n (%)	7 (8.97)	3 (8.82)	0.98
Cons/GGO predominance, n (%)			0.82
Cons	2 (2.56)	2(5.88)	
GGO	75 (96.15)	32 (94.12)	
Equal	1 (1.28)	0	
Cons/GGO distribution, n (%)			0.06
Segmental	6 (7.69)	5 (14.71)	
Non-segmental	6 (7.69)	7 (20.59)	
Lobular	66 (84.62)	22 (64.71)	
TIB, n (%)	5 (6.41)	5 (14.71)	0.16
Bronchial wall thickening, n (%)	27 (34.62)	16 (47.06)	0.21
Reticulation, n (%)	45 (57.69)	18 (52.94)	0.64
LN enlargement, n (%)	5 (6.41)	5 (14.71)	0.16
Pleural effusion, n (%)	8 (10.26)	8 (23.53)	0.07
Cavity	2 (2.56)	0	0.35
Cyst	13 (16.67)	4 (11.76)	0.51

Data are presented as numbers of patients, with percentages in parentheses. PCP = pneumocystis pneumonia, CMV-P = pneumocystis pneumonia, GGO = ground-glass opacity, Cons = consolidation, TIB = tree-in-bud sign, LN = lymph node, NS = no significance.

Table 3
Thoracic CT features with significant differentiating frequency.

	PCP (n = 78)	CMV-P (n = 34)	P-value
Nodule, n (%)	7 (8.97)	16 (47.06)	0.001
Nodule-size, n (%)			0.001
Micro	1 (1.28)	5 (14.71)	
Small	5 (6.41)	11 (32.35)	
Large	1 (1.28)	0	
Nodule-distribution, n (%)			0.001
Centrilobular	3 (3.85)	8 (23.53)	
Perilymphatic	1 (1.28)	0	
Random	3 (3.85)	8(23.53)	
Consolidation, n (%)	28 (35.90)	21 (61.77)	0.01
Halo sign, n (%)	9 (11.54)	11 (32.35)	0.01
Data are presented as numbers of patients, with percentages in parentheses. PCP = pneumocystis pneumonia, CMV-P = pneumocystis pneumonia.			

Table 4
The results of binary logistic regression analysis.

HRCT features	B value	Wald value	Odds Ratio	P-value	95% CI	AUC
Nodules	2.230	16.696	9.298	0.001	3.191–27.095	
Consolidation	1.104	5.417	3.015	0.020	1.190–7.637	0.769
constant	-1.919	24.951	0.147	0.001		
CI = confidence intervals, AUC = area under the receiver operating						

Table 5
Correlation analysis of nodules' occurrence between PCP and CMV-P patients.

	PCP (n = 78)		CMV-P (n = 34)	
variable	R-value	P-value	R-value	P-value
$CD4^+$T cell count	0.159	0.163	0.545	0.001
$CD8^+$T cell count	0.111	0.332	0.392	0.022
CD4/CD8 ratio	0.104	0.366	0.503	0.002
CRP	-0.059	0.607	0.182	0.304
Neutrophil percentage	0.02	0.859	-0.233	0.186
HIV viral load	0.08	0.488	-0.27	0.122
PCP = pneumocystis pneumonia, CMV-P = pneumocystis pneumonia, CRP = C-reactive protein.				

Correlation analysis of nodules' occurrence between PCP and CMV-P patients

We next performed the correlation analysis of nodules' and consolidations' occurrence between PCP and CMV-P patients. Results showed that the nodules' occurrence were positively correlated with $CD4^+$T cell count, $CD8^+$T cell count and CD4/CD8 ratio, while no significant correlations were found with CRP, neutrophil percentage and HIV viral load in CMV-P patients. Among patients with PCP, no significant correlations were observed between nodules' occurrence and clinical indicators. Meanwhile, there were no significant correlations between consolidations' occurrence and clinical indicators in PCP and CMV-P patients (data were not shown).

Discussion

P. jirovecii is an extracellular fungus that almost exclusively inhabits alveolar spaces[15], causing pulmonary infection through adhesion to the surface of alveolar epithelium cells (type I pneumocytes) [16]. CMV belongs to the herpes viridae family, with seroprevalence of 40%–100% approximately in the world's population [4, 17], which could establish life-long infection and reactivate during episodes of immunosuppression [18]. The cell-mediated immunodeficiency is particularly essential for the development of PCP and CMV-P. PCP (approximately 90% cases) usually occurs with CD4 lymphocyte counts < 200 cells/mm^3, while CMV-P tends to occur with $CD4^+$ T lymphocyte counts 50 cells/mm^3 [19]. The results of present study showed that $CD4^+$ T lymphocyte counts of PCP group and CMV-P group were both lower than 50 cells/mm^3 (22 and 22.50 cells/mm^3,respectively), which were consistent with previous studies. Nevertheless, our data also demonstrated that the neutrophil percentage in PCP was higher than in CMV-P, while the lymphocyte percentage in CMV-P was higher than in PCP, this were consistent with previous studies as well [20].

The identification between PCP and CMV-P is particularly challenging since clinical characteristics are similar in both groups. As P. jirovecii is difficult to cultivate in vitro, the diagnosis usually established with identification of the pathogen in respiratory specimens (BAL fluid ideally or induced sputum otherwise) by sensitive immunocytochemical methods or polymerase chain reaction (PCR) [8–10]. In this study, we diagnosed PCP when clinical features were present combined with P. jirovecii were detected by silver stain or PAS in a BAL fluid. With regard to CMV-P, a diagnosis requires clinical symptoms of pulmonary infection combined with identification of CMV in lung biopsy or BAL fluid by rapid culture, viral isolation, immunohistochemistry, histopathology, or DNA hybridization techniques [11]. In the current study, the diagnosis of CMV-P were established when clinical evidence for infection coinciding with definitive BAL results of fluorescence quantitative PCR. However, Microbiological confirmation is usually invasive or difficult to obtain, which may have delayed the diagnosis and initiation of therapies. To identify the differences between these two pathogens in radiological features, we retrospectively compared the HRCT features in 78 patients with PCP and in 34 patients with CMV-P.

Our data showed that the frequency of GGO were significantly common, while the occurrence of cavity was relatively rare in both cohorts. Meanwhile, among patients with PCP and CMV-P, the frequency of reticulation, bronchial wall thickening, mosaic perfusion, cyst, crazy-paving pattern, TIB, and LN enlargement are similar to each other. These findings are in accordance with previous studies concerning infections in immunocompromised patients[21]. Kunihiro et al demonstrated that representative CT features in immunosuppressed patients included diffuse GGO with mosaic pattern in PCP and nodules with or without the halo sign in CMV-P[22]. PCP was reported to have variable atypical CT features; 18% of PCP patients accompany LN enlargement, 3%-5% show nodular lesions [23]. Concerning CMV-P, a mixed pattern with GGO, consolidation, and nodules was observed to its common CT features in previous studies of AIDS patients [21].This would suggest that there are several similarities in CT features between these two types of pneumonia.

In the current study, the comparisons made between PCP and CMV-P showed that the occurrence of consolidation, nodules, and the halo sign is more common in CMV-P than in PCP. In addition, large nodules with perilymphatic distribution were not found in any of patients with CMV-P group. In addition, the nodules' occurrence were positively correlated with $CD4^+$T cell count, $CD8^+$T cell count and CD4/CD8 ratio in CMV-P patient, while no significant correlations were found in PCP patients. These similarities and differences in CT features may be correlated to the histopathology in each type of pneumonia. The primary histopathological feature of PCP and CMV-P is diffuse alveolar damage [24, 25]. GGO and reticulation represent the pathological features of diffuse alveolar damage [26, 27]. Thus, CT features of GGO and reticulation appearance are common in both groups. However, some studies suggest that the pulmonary injury of PCP is induced by exuberant inflammation[28], while the lung damage of CMV-P appears to be the direct result by the cytopathogenic effects of CMV in AIDS patients[29]. Consolidation refers to advanced stages of the inflammation in which the alveoli are filled with exudates or other product, rendering the lung solid[30]. Considering the differences in immune status and viral loads between the two cohorts, consolidation in patients with CMV-P should be more frequently observed than

with PCP. Nodule was reported as a common CT finding in patients with CMV-P[29]. Pathologically, nodules corresponding to areas of hemorrhagic or inflammatory nodules indicate the intraalveolar aggregations of red blood cells, macrophages, and fibrin [29]. Hypotheses have been assumed to interpret the mechanism of rare nodules in PCP including microorganism factors, the absence of IgA Pneumocystis antibodies and change in CD4 T cell [31–33]. It is reported that the halo-sign was observed in approximately 60% of viral etiology cases. Finding multiple nodules smaller than 10 mm in appropriate clinical scenario have a sensitivity, specificity, and negative predicted value for viral infection of greater than 80%[34].

There are several limitations in present study. The patients included were in different stages of diseases because of using the BAL results as diagnostic criteria, which might influenced the observed frequency of CT features, such as halo signs and cavities. The lack of histological specimens limited the analysis of correlation with pathologic radiology. The analysis of correlation between histology and pathologic radiology was limited owing to the lack of histological specimens. In addition, sensitivity and specificity of these patterns in AIDS patients should be further evaluated in a blinded retrospective or future prospective study.

Conclusions

The occurrence of consolidation, micro and small nodules with centrilobular or random distribution, and halo sign were highly suggestive of CMV-P rather than PCP in AIDS patients. The GGO, reticulation, and bronchial wall thickening were found similar occurrence in both pneumonia and, hence, can't contribute to differentiate the two diseases.

Abbreviations

HRCT
High-resolution computed tomography; AIDS:Acquired immunodeficiency syndrome; PCP Pneumocystis pneumonia; CMV-P:Cytomegalovirus pneumonia; GGO:Ground-glass opacity; TIB:Tree-in-bud sign; BAL:Bronchoalveolar lavage; P. jirovecii:Pneumocystis jirovecii; LN:Lymph node
CI
Confidence intervals; AUC:Area under the receiver operating

Declarations

Availability of data and materials

Data of the study can be available upon request from the author.

Ethics approval and consent to participate

This clinical study was conducted in compliance with the ethical principles of the Declaration of Helsinki and its later amendments. The Ethics Committee of Beijing Ditan Hospital approved our study protocol [approval no. NA2018(005)-01]. As a de-identified retrospective study, the ethics committee did not require us to obtain written or verbal informed consent from participants.

Consent for publication

Not applicable.

Competing interests

The authors declare that they have no competing interests.

Funding

This study has received funding by Beijing Municipal Administration of Hospitals Clinical Medicine Development of Special Funding Support (CN), China [Grant No: ZYLX201802].

Authors' contributions

Conception and design: Ang Li, Budong Chen. Performed the experiments: Chunjing Du, Ang Li, Budong Chen, Jingyuan Liu, Hui Chen, Lin Pu, Ming Zhang. Analyzed the data: Chunjing Du, Ang Li, Budong Chen. Contributed materials/analysis tools: Chunjing Du, Ang Li, Budong Chen. Wrote the paper: Chunjing Du, Ang Li, Budong Chen. All authors read and approved the final manuscript.

Acknowledgements

The authors gratefully acknowledge Liuluan Zhu Ph.D., and Hui Zeng Ph.D. for their assistance with experiments designed, as well as Gang Wan Ph.D. and Junnan Li Ph.D. for their assistance with data analysis.

References

1. Bhutta ZA, Sommerfeld J, Lassi ZS, et al. Global burden, distribution, and interventions for infectious diseases of poverty[J]. Infect Dis Poverty. 2014;3:21.
2. Knoblauch AM, Divall MJ, Owuor M, et al. Experience and lessons from health impact assessment guiding prevention and control of HIV/AIDS in a copper mine project, northwestern Zambia[J]. Infect Dis Poverty. 2017;6(1):114.
3. Mckinnell JA, Cannella AP, Kunz DF, et al. Pneumocystis pneumonia in hospitalized patients: a detailed examination of symptoms, management, and outcomes in human immunodeficiency virus

(HIV)-infected and HIV-uninfected persons[J]. Transpl Infect Dis. 2012;14(5):510–8.

4. Fonseca Brito L, Brune W, Stahl FR. Cytomegalovirus (CMV) Pneumonitis: Cell Tropism, Inflammation, and Immunity[J]. Int J Mol Sci. 2019;20(16):3865.
5. Gigliotti F, Wright TW. Pneumocystis: where does it live?[J]. PLoS Pathog. 2012;8(11):e1003025.
6. Sepkowitz KA. Opportunistic infections in patients with and patients without Acquired Immunodeficiency Syndrome[J]. Clin Infect Dis. 2002;34(8):1098–107.
7. Nichols WG, Boeckh M. Recent advances in the therapy and prevention of CMV infections[J]. J Clin Virol. 2000;16(1):25–40.
8. Cooley L, Dendle C, Wolf J, et al. Consensus guidelines for diagnosis, prophylaxis and management of Pneumocystis jirovecii pneumonia in patients with haematological and solid malignancies, 2014[J]. Intern Med J. 2014;44(12b):1350–63.
9. Doyle L, Vogel S, Procop GW. Pneumocystis PCR. It Is Time to Make PCR the Test of Choice[J]. Open Forum Infect Dis. 2017;4(4):x193.
10. Procop GW, Haddad S, Quinn J, et al. Detection of Pneumocystis jiroveci in respiratory specimens by four staining methods[J]. J Clin Microbiol. 2004;42(7):3333–5.
11. Ljungman P, Boeckh M, Hirsch HH, et al. Definitions of Cytomegalovirus Infection and Disease in Transplant Patients for Use in Clinical Trials[J]. Clin Infect Dis. 2017;64(1):87–91.
12. Razonable RR, Hayden RT. Clinical utility of viral load in management of cytomegalovirus infection after solid organ transplantation[J]. Clin Microbiol Rev. 2013;26(4):703–27.
13. Chuganji E, Abe T, Kobayashi H, et al. Fatal Pulmonary Co-infection with Pneumocystis and Cytomegalovirus in a Patient with Acquired Immunodeficiency Syndrome[J]. Intern Med. 2014;53(14):1575–8.
14. Cereser L, Dallorto A, Candoni A, et al. Pneumocystis jirovecii pneumonia at chest High-resolution Computed Tomography (HRCT) in non-HIV immunocompromised patients: Spectrum of findings and mimickers[J]. Eur J Radiol. 2019;116:116–27.
15. Skalski JH, Kottom TJ, Limper AH. Pathobiology of Pneumocystis pneumonia: life cycle, cell wall and cell signal transduction[J]. FEMS Yeast Res. 2015, 15(6).
16. Avino LJ, Naylor SM, Roecker AM. Pneumocystis jirovecii Pneumonia in the Non-HIV-Infected Population[J]. Ann Pharmacother. 2016;50(8):673–9.
17. Omeri AK, Okada F, Takata S, et al. Comparison of high-resolution computed tomography findings between Pseudomonas aeruginosa pneumonia and Cytomegalovirus pneumonia[J]. Eur Radiol. 2014;24(12):3251–9.
18. Lee HS, Park JY, Shin SH, et al. Herpesviridae viral infections after chemotherapy without antiviral prophylaxis in patients with malignant lymphoma: incidence and risk factors[J]. Am J Clin Oncol. 2012;35(2):146–50.
19. Ahuja J, Kanne JP. Thoracic infections in immunocompromised patients[J]. Radiol Clin North Am. 2014;52(1):121–36.

20. Youssef J, Novosad SA, Winthrop KL. Infection Risk and Safety of Corticosteroid Use[J]. Rheumatic Disease Clinics of North America. 2016;42(1):157–76.
21. Gasparetto EL, Ono SE, Escuissato D, et al. Cytomegalovirus pneumonia after bone marrow transplantation: high resolution CT findings[J]. Br J Radiol. 2004;77(921):724–7.
22. Kunihiro Y, Tanaka N, Kawano R, et al. Differential diagnosis of pulmonary infections in immunocompromised patients using high-resolution computed tomography[J]. Eur Radiol. 2019;29(11):6089–99.
23. Boiselle PM, Crans CJ, Kaplan MA. The changing face of Pneumocystis carinii pneumonia in AIDS patients[J]. AJR Am J Roentgenol. 1999;172(5):1301–9.
24. Kayik SK, Acar E, Memis L. Pneumocystis Jirovecii Pneumonia in Newly Diagnosed HIV Infection: A Challenging Case Report[J]. Turk Patoloji Derg. 2020, 1(1).
25. Mcguinness G, Scholes JV, Garay SM, et al. Cytomegalovirus pneumonitis: spectrum of parenchymal CT findings with pathologic correlation in 21 AIDS patients[J]. Radiology. 1994;192(2):451–9.
26. Ichikado K, Suga M, Gushima Y, et al. Hyperoxia-induced diffuse alveolar damage in pigs: correlation between thin-section CT and histopathologic findings[J]. Radiology. 2000;216(2):531–8.
27. Marchiori E, Muller NL, Soares SAJ, et al. Pulmonary disease in patients with AIDS: high-resolution CT and pathologic findings[J]. AJR Am J Roentgenol. 2005;184(3):757–64.
28. Thomas CJ, Limper AH. Pneumocystis pneumonia[J]. N Engl J Med. 2004;350(24):2487–98.
29. Kim EA, Lee KS, Primack SL, et al. Viral pneumonias in adults: radiologic and pathologic findings[J]. Radiographics. 2002, 22 Spec No: S137-S149.
30. Hansell DM, Bankier AA, Macmahon H, et al. Fleischner Society: glossary of terms for thoracic imaging[J]. Radiology. 2008;246(3):697–722.
31. Hartel PH, Shilo K, Klassen-Fischer M, et al. Granulomatous reaction to pneumocystis jirovecii: clinicopathologic review of 20 cases[J]. Am J Surg Pathol. 2010;34(5):730–4.
32. Otahbachi M, Nugent K, Buscemi D. Granulomatous Pneumocystis jiroveci Pneumonia in a patient with chronic lymphocytic leukemia: a literature review and hypothesis on pathogenesis[J]. Am J Med Sci. 2007;333(2):131–5.
33. Totet A, Duwat H, Daste G, et al. Pneumocystis jirovecii genotypes and granulomatous pneumocystosis[J]. Med Mal Infect. 2006;36(4):229–31.
34. Raoof S, Raoof S, Naidich DP. Imaging of unusual diffuse lung diseases[J]. Curr Opin Pulm Med. 2004;10(5):383–9.

Figures

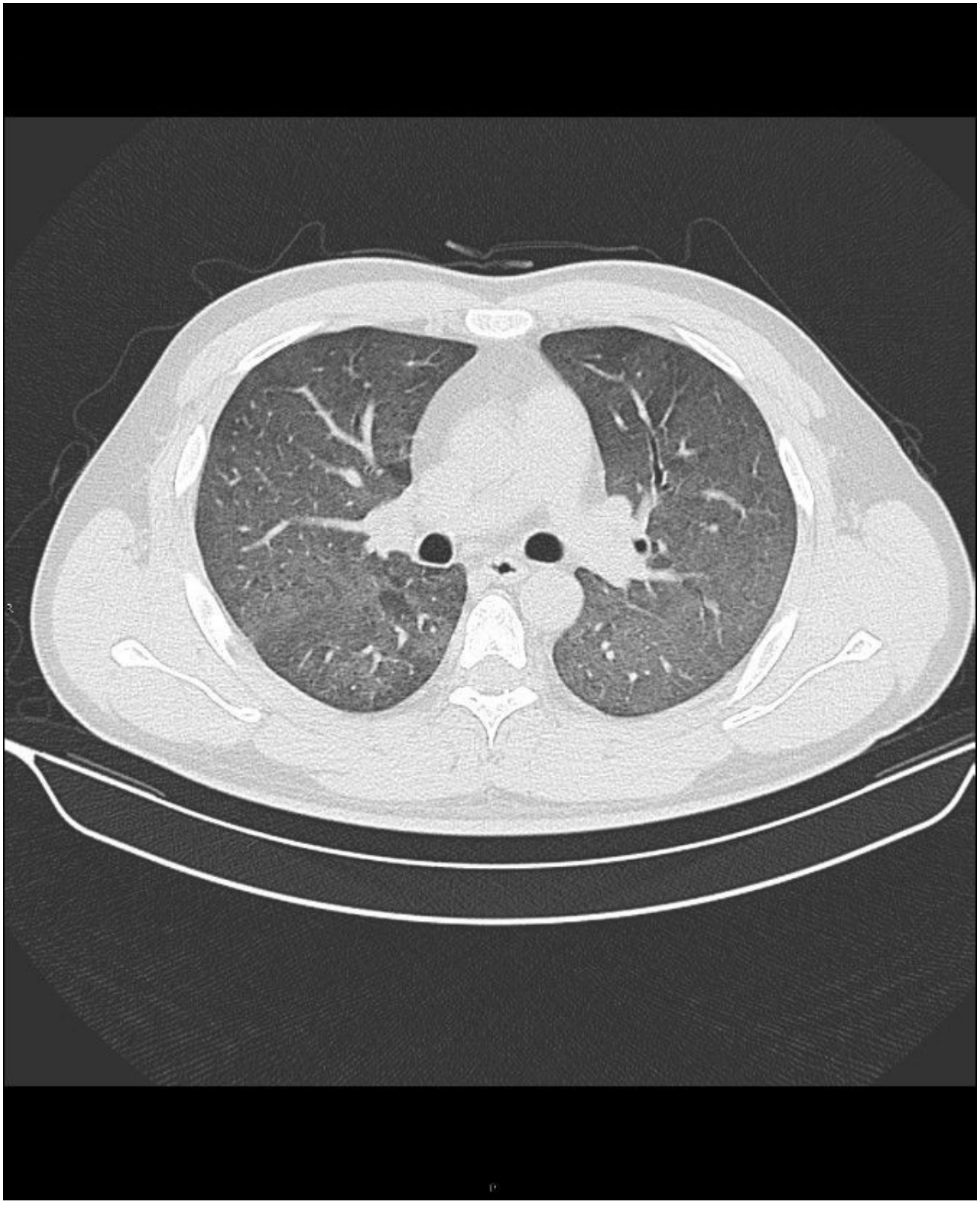

Figure 1

Pneumonia caused by P. jirovecii in a 28-year-old male patient with AIDS. HRCT image showed diffuse ground-glass opacity of bilateral pulmonary parenchyma.

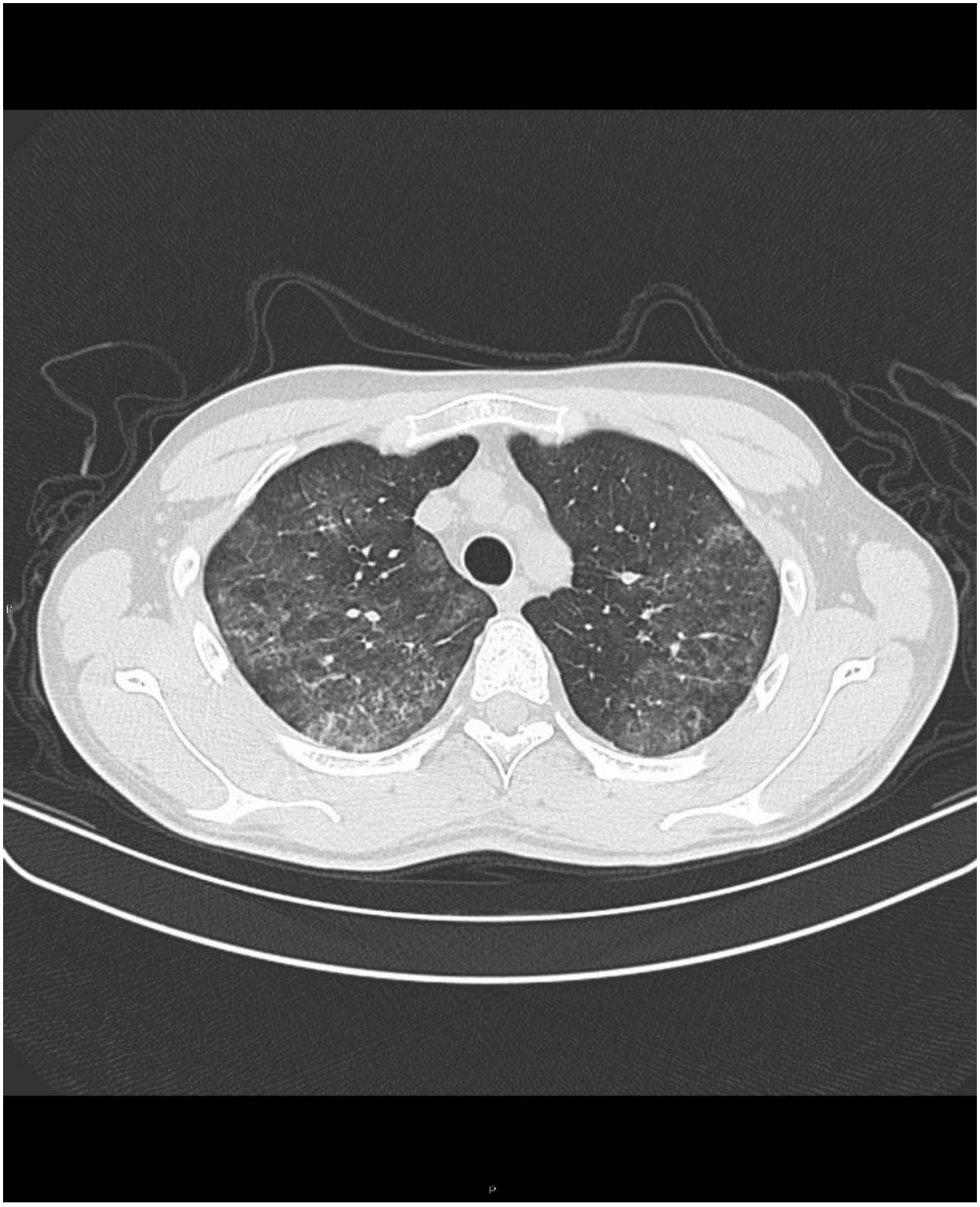

Figure 2

Pneumonia caused by P. jirovecii in a 31-year-old male patient with AIDS. HRCT image showed multiple ground-glass opacity of bilateral pulmonary parenchyma with reticulate changes.

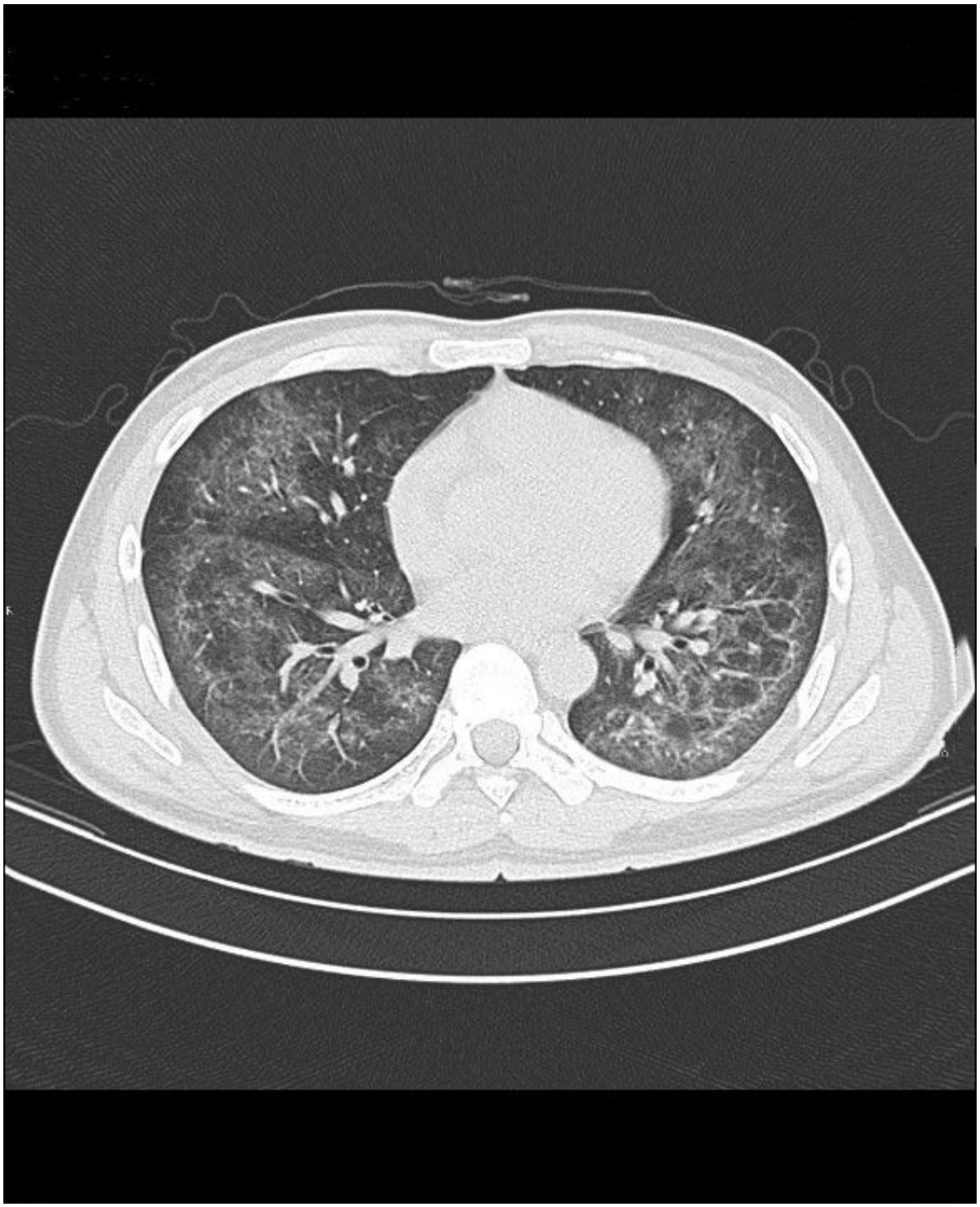

Figure 3

Pneumonia caused by CMV in a 38-year-old male patient with AIDS. HRCT image showed ground-glass opacity, reticulation, and mosaic perfusion.

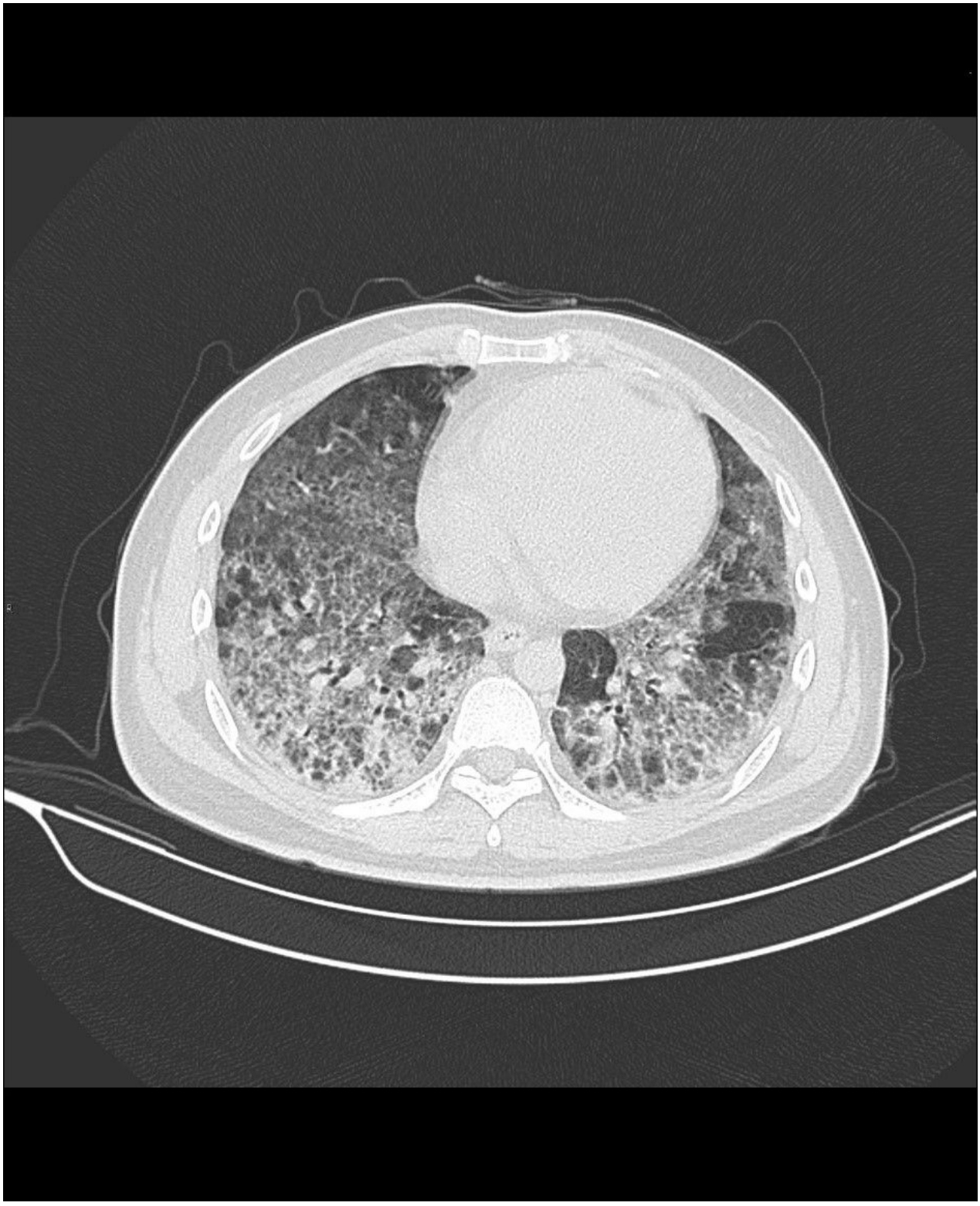

Figure 4

Pneumonia caused by CMV in a 36-year-old male patient with AIDS. HRCT image showed ground-glass opacity, reticulation, consolidation, and mosaic perfusion.

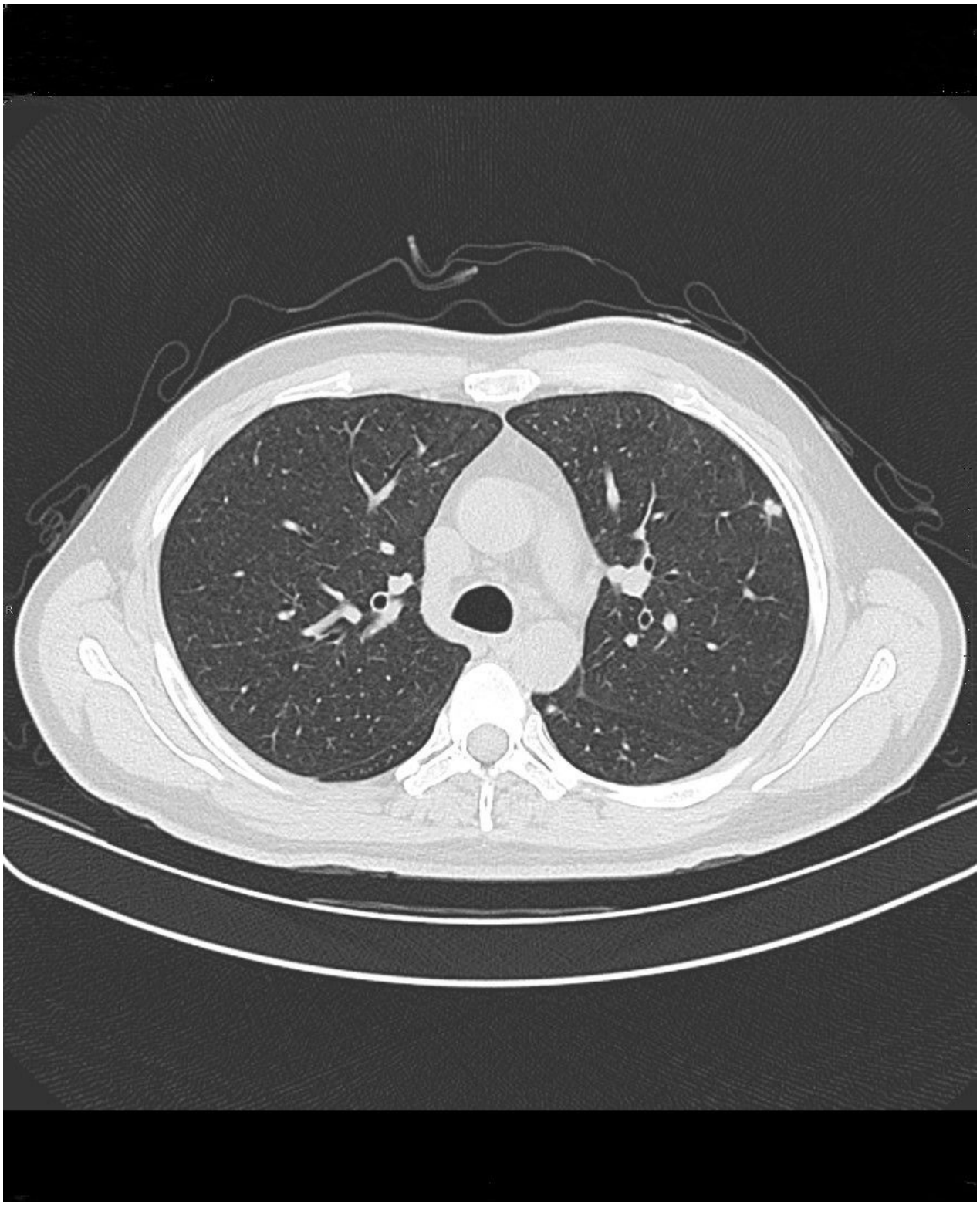

Figure 5

Pneumonia caused by CMV in a 29-year-old male patient with AIDS. HRCT image showed ground-glass opacity, nodules with halo sign and tree in bud sign.